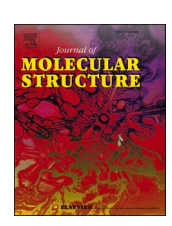
ELSEVIER

Contents lists available at ScienceDirect

Journal of Molecular Structure

journal homepage: www.elsevier.com/locate/molstr





Visible light driven photocatalytic and competent antioxidant properties of phyto-fabricated zinc oxide nanoparticles (ZnO-NPs) from *Borreria hispida*

Abhilash Mavinakere Ramesh ^a, Dhananjay Purushotham ^b, Anju Kodandaram ^a, Natarajamurthy Shilpa ^c, Sudarshana Brijesh Singh ^d, Mohammed Aiyaz ^e, Hittanahallikoppal Gajendramurthy Gowtham ^f, Abbas Rahdar ^g, Kasinathan Kaviyarasu ^{h,i,*}, Mahadevamurthy Murali ^{d,*}

- a Department of Studies in Environmental Science, University of Mysore, Manasagangotri, Mysore 570006, India
- ^b Centre for Materials Science and Technology, Vijyana Bhavan, University of Mysore, Mysore 570006, India
- ^c Department of Studies in Microbiology, University of Mysore, Manasagangotri, Mysore, Karnataka 570006, India
- ^d Department of Studies in Botany, University of Mysore, Manasagangotri, Mysore, Karnataka 570006, India
- ^e Department of Studies in Biotechnology, University of Mysore, Manasagangotri, Mysore, Karnataka 570006, India
- f Department of PG Studies in Biotechnology, Nrupathunga University, Nrupathunga Road, Bangalore 560001, India
- g Department of Physics, Faculty of Science, University of Zabol, Zabol 98613-35856, Iran
- h UNESCO-UNISA Africa Chair in Nanosciences/Nanotechnology Laboratories, College of Graduate Studies, University of South Africa (UNISA), Muckleneuk Ridge, PO Box 392, Pretoria, South Africa
- i Nanosciences African Network (NANOAFNET), Materials Research Group (MRG), iThemba LABS-National Research Foundation (NRF), 1 Old Faure Road, 7129, PO Box 722. SomersetWest. Western Cape Province. South Africa

ARTICLE INFO

Keywords: ZnO-NPs Borreria hispida Antioxidant Methyl red Dye degradation

ABSTRACT

Zinc oxide nanoparticles (ZnO-NPs) have gained considerable interest in biological and photocatalytic applications due to their distinctive physico-chemical characteristics. The study aimed to synthesize ZnO-NPs using the leaf extract of Borreria hispida, a medicinally important plant for its antioxidant and photocatalytic efficacy. The B. hispida mediated ZnO-NPs (Bh-ZnO-NPs) illustrated a characteristic peak at 304 nm with 3.45 eV bandgap energy during the spectral analysis. The Bh-ZnO-NPs XRD studies revealed stiff and narrow peaks with $\sim\!21.87$ nm in size. The SEM analysis revealed that the obtained Bh-ZnO-NPs were agglomerated and ZnO elemental purity of 98.23% was confirmed through EDS. The spectral results of Bh-ZnO-NPs obtained by the FT-IR affirmed that phyto-constituents participated in the reduction, capping and stabilization of the particles during the synthesis of nanoparticles. The BET surface area analysis of the Bh-ZnO-NPs confirmed that the particles exhibit a similar Type - IV isotherm curve as per IUPAC classification with 11.681 m² g⁻¹ and a surface roughness (Ra) value of 6.25 nm. The Bh-ZnO-NPs offered significant ($p \le 0.05$) radical scavenging activity, which was dosedependent with IC_{50} value falling between 0.6 to 0.8 mg mL⁻¹ among the evaluated test methods. Methyl red (MR) dye degradation tests employing phyto-fabricated Bh-ZnO-NPs resulted in dye degradation up to 94.22% after 40 min of solar irradiation and the decolorization of MR dye followed pseudo-first-order kinetics. In addition to those mentioned above, the fifth cycle of the photocatalyst's stability and reusability studies showed 84.8% dye degradation ability. The findings demonstrate that the phyto-fabricated ZnO-NPs from B. hispida have potent antioxidant and dye-degrading properties that can be investigated at an industrial scale.

1. Introduction

Nanotechnology is one amongst the most researched fields in current times that deal with the manipulation of matter at the nanometre scale, resulting in the creation of novel materials with unique properties of importance [1–3]. Irrespective of the technique employed in synthesizing nanoparticles (physical, chemical or biological), it had resulted in the improvement of one or the other properties, viz., chemical, physical, mechanical or biological properties of the particles that emerged when the matter was structured at the nanoscale, thereby also termed as "a

E-mail addresses: kavi@tlabs.ac.za (K. Kaviyarasu), botany.murali@gmail.com (M. Murali).

^{*} Corresponding authors.

wonder of modern medicine" [4–7] The quick pace in synthesizing these nanoparticles for specific applications in the recent past has resulted in perceiving these particles in almost all fields of life, including healthcare and environmental protection [8–10].

Numerous nanoparticles of metal/metal oxide forms are being synthesized and studied for diverse physico-chemical and biological applications [11–14]. Among the many forms of nanoparticles, owing to their distinctiveness, zinc oxide nanoparticles (ZnO-NPs) are deemed to be nontoxic, biocompatible, and safe, allowing for their application in various biological and pharmaceutical applications [15–18]. Apart from the above, they are also attractive owing to their distinctive physico-chemical characteristics: a wide band gap, high piezoelectricity, and high binding energy. It has been noted that the surface of zinc oxide is rich in hydroxyl (-OH) groups that allow them to dissolve even under acid and strong basic conditions [19,20].

As noted earlier, many methods are employed for synthesizing ZnO-NPs. Among them, the biological route is renowned for being economical and environmentally friendly in comparison to the chemical method that produces toxic by-products, thereby depicting them as unsafe for biological and environmental purposes [21]. The different sources (chemical and biological origin) used in synthesizing ZnO-NPs for their exploitation in various physical and biological applications are owed to their distinctive and beneficial properties [22]. Of the various biological sources used in synthesizing ZnO-NPs, plant extracts are advantageous over their counterparts by being easily available and safe to handle. ZnO-NPs are biosynthesized from metal-based precursors using plant extracts, and this process typically entails the reaction of the two in which the phyto-constituents of the extract act as reducing, capping and stabilizing agents that facilitate in reduction of metal-based precursors that act as oxidizing agents to form metal-based NPs [5,20,23].

Besides, ZnO-NPs are well recognized for their efficient application in eliminating toxigenic dyes from industrial wastewater as they are known to be non-degradable and cause pollution to the ecosystem [24, 25]. When contaminating the water body, these dyes prevent light from penetrating the water, affecting the aquatic environment's biological balance, death of aquatic life, and even causing human health problems [26]. Many industries employ major effluent dyes as coloring agents, including methyl red, which is low cost and has great coloring effectiveness in small-scale industries [27]. Additionally, phyto-syntheiszed ZnO-NPs (using plants) have been known to readily and effectively degrade the dyes and utilization of these nanoparticles are of great alternative to the present-day applications [25,28]. To date, numerous plant species, irrespective of their parts, for extraction with various solvents are utilized for synthesizing ZnO-NPs, which possess biological and environmentally friendly applications [2,16]. But still, a considerable gap has been left and to overcome there is a need to identify potential new materials with multiple applications, including biological and photocatalytic properties. Borreia hispida (Rubiaceae) is well known for its medicinal importance from ancient times, including Siddha medicine. It has been explored for various biological properties like antidiabetic, antihypertensive, antihyperlipidemic, hepatoprotective,

2. Materials and methods

2.1. Phyto-fabrication of ZnO-NPs

Healthy *Borreriahispida*leaves were obtained from Mysuru, Karnataka, India. The leaves from the plants were carefully trimmed and rinsed with tap and distilled water (DW) followed by blot dry. The leaf material (25 gm) was ground in Waring blender with DW (100 mL), subjected to agitation for 2 h at 100 rpm on a rotary shaker, and filtered. About 100 mL of plant extract was heated up to 60 to 80 °C on a magnetic stirrer and the zinc nitrate hexahydrate (10 g) was introduced (little by little). The process continued until the mixture became paste or reduced to 5 mL and transferred to a silica crucible, then subjected to calcination at 300 °C for 2 h in a silica crucible [32]. The resultant powder was considered ZnO-NPs (Bh-ZnO-NPs) and used for further experiments.

2.2. Physico-chemical characterization of phyto-fabricatedBh-ZnO-NPs

The synthesized particles were characterized for their physicchemical nature through various techniques. The phyto-fabricated particles were subjected to UV-vis spectral analysis to determine their absorbance spectra between 200 and 800 nm using a spectrophotometer (Beckman Coulter, Germany) followed by energy bandgap calculation by Tauc's plot. The X-Ray Diffraction (XRD) studies of the phytofabricated particles were analyzed on a Rigaku SmartLab (Tokyo). The surface morphology of the Bh-ZnO-NPs was observed using FE-SEM (HITACHI, USA), followed by elemental analysis through energy dispersive spectroscopy (EDS) (Zeiss Supra 55VP, Japan). To determine the size of the Bh-ZnO-NPs high-resolution- transmission electron microscopy (HR-TEM) examination was performed using Jeol/JEM-2100 (Japan). The changes in the binding affinities throughout the synthesis process of Bh-ZnO-NPs were assessed using Fourier Transform-Infrared (FT-IR) Spectroscopy (Perkin Elmer Spectrum 1000). The-Braunauer-Emmett-Teller (BET) studies of the particles were analyzed using BEL:2 SORP (Italy).

2.3. Antioxidant response of Bh-ZnO-NPs

The radical scavenging activity (RSA) of Bh-ZnO-NPs was carried out by different methods viz., 2,2-diphenyl-1-picrylhydrazyl (DPPH), ABTS, Hydrogen Peroxide and Superoxide Radical Scavenging Assays [33]. In brief, the obtained nanoparticles (Bh-ZnO-NPs) was to 5 mL of 0.1 mM DPPH (in methanol) at various concentrations (0.2 to 1 mg mL $^{-1}$) individually and thoroughly mixed before subjecting to incubation at different time intervals according to the method employed under dark. The percentage of RSA in the tested samples was computed using spectroscopic measurements of the incubated samples.

Radical Scavenging Activity (%) = $\frac{\text{Absorbance of Control} - \text{Absorbance of Test sample}}{\text{Absorbance of Control}} \times 100$

antifungal, anti-inflammatory, anticancer, anticataract, etc. [29,30]. Besides, the plant has been utilized in synthesizing copper oxide nanoparticles with potential antioxidant properties [31] and there are no other reports on the utilization of the plants of the genus *Borreria*. Hence a study was planned to explore the potential of *B. hispida*, which has many medicinal properties for phyto-fabrication of ZnO-NPs and evaluate its antioxidant and photocatalytic potentiality.

2.4. Photocatalytic response of Bh-ZnO-NPs

The methyl red dye degradation studies were performed by employing biosynthesized Bh-ZnO-NPs under solar irradiation (430–790 THz) as per the protocol designed by Abhilash et al. [25]. During the study, Bh-ZnO-NPs were first allowed to react with 10 mg $\rm L^{-1}$ of MR dye in a flask at various concentrations (0.2 to 1 g $\rm L^{-1}$) to determine their dye degradation capacity. Under solar illumination, the reaction flasks were

continually agitated on a magnetic stirrer and the absorbance was taken every 10 min to assess the Bh-ZnO-NPs' dye degradation capacity [34]. A pseudo-first-order kinetic model was illustrated to note the connection between adsorption and photo-degradation in solid-liquid systems. The experimental values were fitted with the rate equation as given below.

$$-\ln(C_t/C_o) = k(p) \times t$$

where C_{t^-} absorbance of MR at t time; C_{o^-} absorbance of MR after dark adsorption; t- irradiationtime; k(p)- pragmatic kinetic rate constant; $kp \, (min^{-1})$ was calculatedfrom the slope of $ln(C_t/C_o)$ versus irradiation time (t).

2.5. Photo-stability and reusability of Bh-ZnO-NPs

Under the same experimental circumstances, the reusability and stability of Bh-ZnO-NPs for the photocatalytic degradation of MR were also evaluated. After the first round of MR dye degradation, the catalyst

was recovered through centrifugation, washed with DW and subjected to drying for 6 h at 80 $^{\circ}$ C. The dried particles were again used as a catalyst for the second run and the method was followed for subsequent utilization for the dye degradation process.

3. Results and discussion

3.1. Physico-chemical characterization of Bh-ZnO-NPs

The UV- visible spectral studies of ZnO-NPs phyto-fabricated using the leaf extract of *B. hispida* showed a peak at 304 nm (Fig. 1A), a distinguishing feature of ZnO-NPs [35], with 3.45 eV bandgap energy (Fig. 1B) based on the spectral data. The results are confirmatory with many findings where it was noted that the ZnO-NPs synthesized, irrespective of the source used in the biological route, will show an absorption peak between UV- A and UV-B regions with an energy band gap between 2.6 to 3.5 eV, which helps in their application in physico-chemical and biological fields [25,32]. The XRD analysis

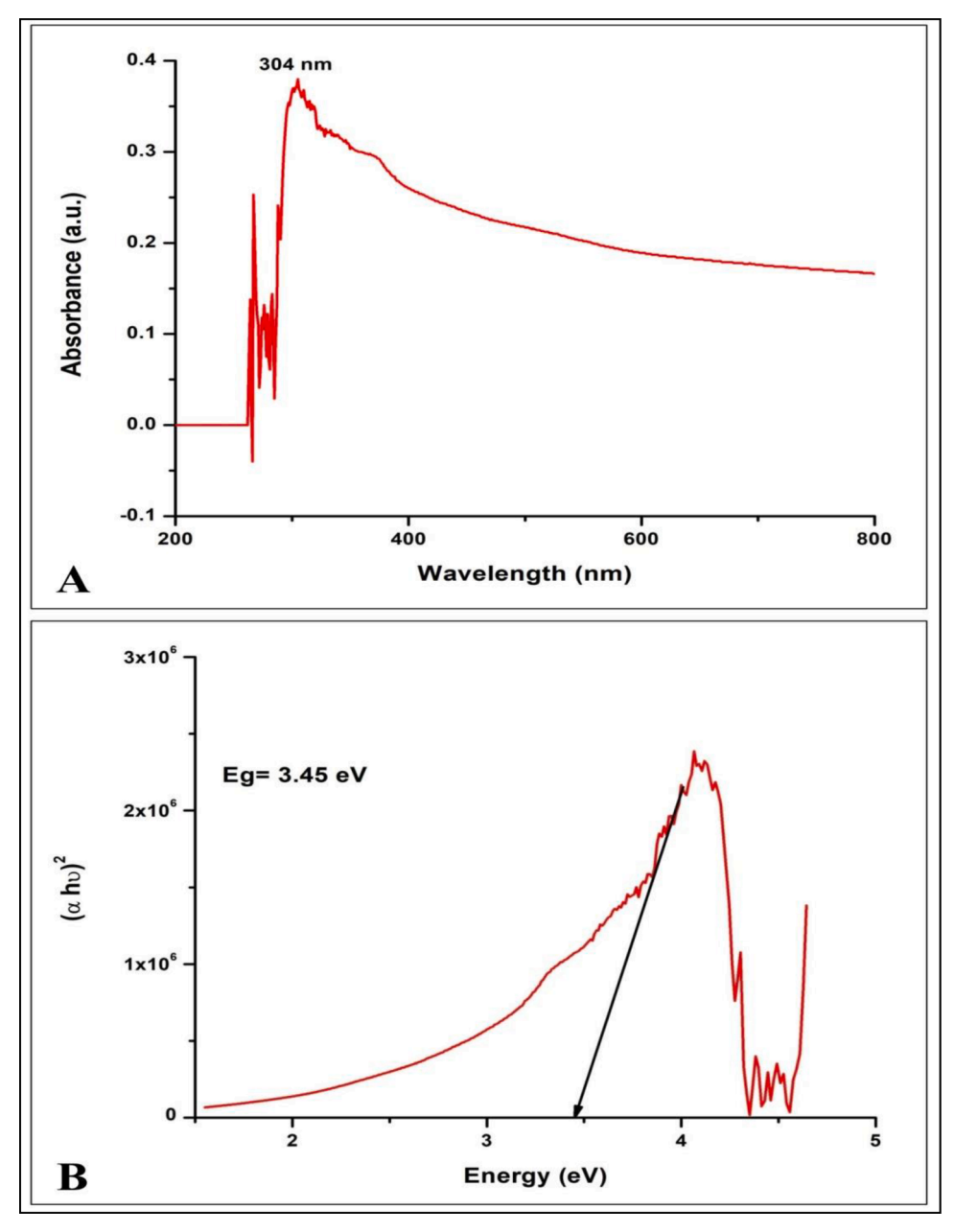


Fig. 1. UV-visible spectra (A) and Tauc's Plot depicting the band-gap energy (B) of phyto-fabricated Bh-ZnO-NPs.

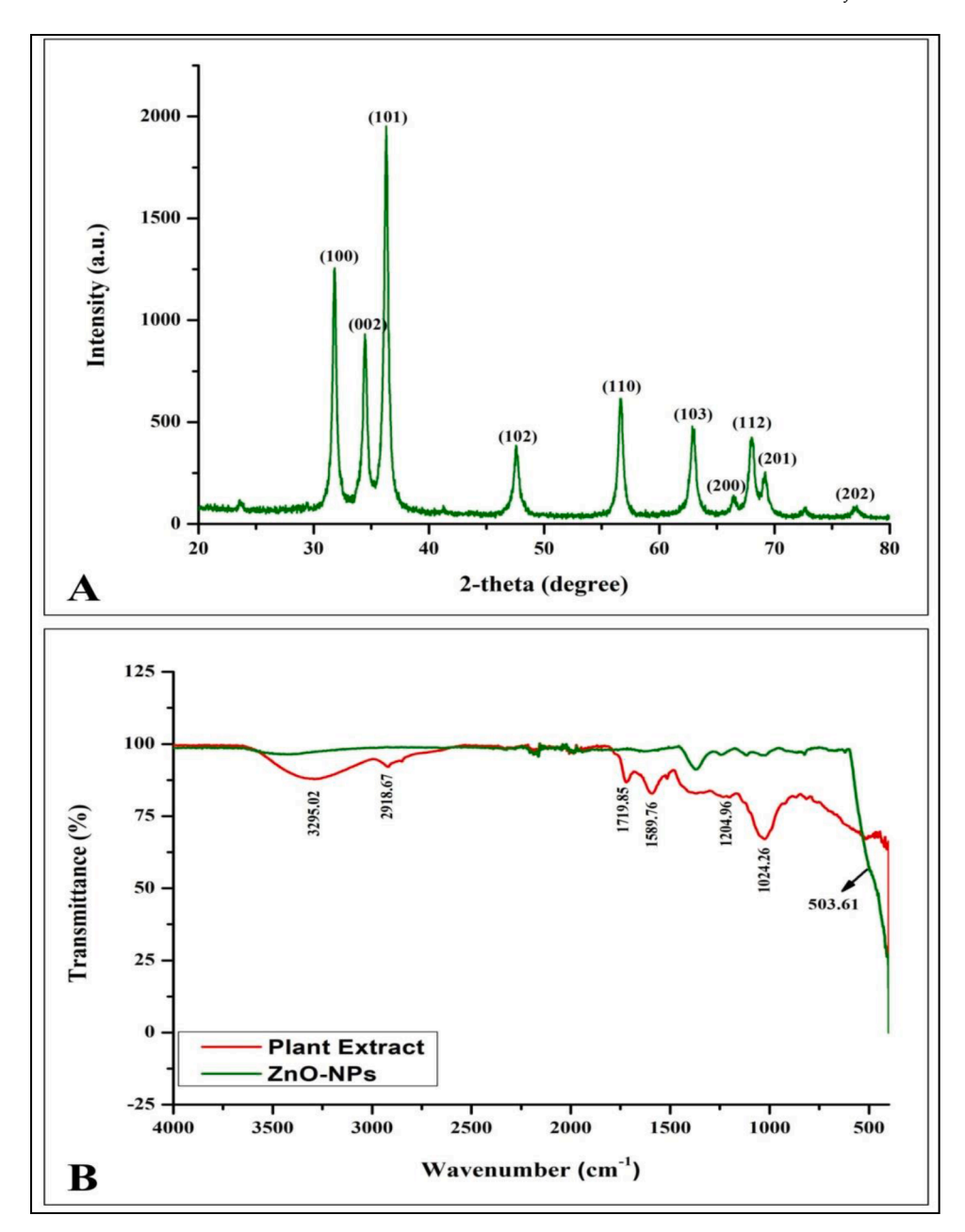


Fig. 2. XRD plot (A) and FT-IR spectra (B) of phyto-fabricated Bh-ZnO-NPs.

Table 1Antioxidant potential of phyto-fabricated Bh-ZnO-NPs.

Antioxidant Assays	$ZnO-NPs (mg mL^{-1})$						
	0.2	0.4	0.6	0.8	1.0		
DPPH	09.02 ± 0.35^{a}	30.41 ± 0.76^{a}	46.86 ± 1.08^{a}	$62.22 \pm 0.74^{\rm a}$	66.78 ± 0.86^{a}		
ABTS	04.61 ± 0.51^{c}	25.51 ± 0.45^{b}	$39.62\pm0.67^{\mathrm{b}}$	$56.27 \pm 0.82^{\rm b}$	61.24 ± 0.63^{bc}		
Superoxide	10.48 ± 0.41^a	30.40 ± 0.49^{a}	$41.62 \pm 0.67^{\rm b}$	50.37 ± 0.51^{c}	59.57 ± 0.42^{c}		
H_2O_2	07.36 ± 0.32^b	28.34 ± 1.03^a	38.04 ± 1.06^{b}	51.51 ± 0.47^c	62.73 ± 0.57^{b}		

Values are the mean of three independent replicates (n=3) and \pm indicates standard error. Means followed by the same letter(s) within the same column are not significantly ($p \le 0.05$) different according to Tukey's HSD.

performed revealed ten noticeable peaks at 31.81° , 34.50° , 36.31° , 47.54° , 56.65° , 62.93° , 66.42° , 68.00° , 69.16° and 77.10° at 2θ angles, which well corresponded to planes of wurtzite shape (Fig. 2A) with a size of \sim 21.87 nm calculated via Scherrer's formula (Suppl. Table 1). The planes noticed during the study were in perfect match with JCPDS No: 85–510 and the stiff and narrow peaks indicate the synthesized

particles had no contaminants, which supports the conclusions of other researchers [21,36]. The FT-IR spectroscopic study was employed to determine whether the phyto-constituents were involved during the reduction, capping and stabilizing of Bh-ZnO-NPs and it was observed that a spectrum band was noted at 503.61 cm⁻¹, corresponding to the metal oxide bond. Likewise, spectrum bands at 3995.02 cm⁻¹

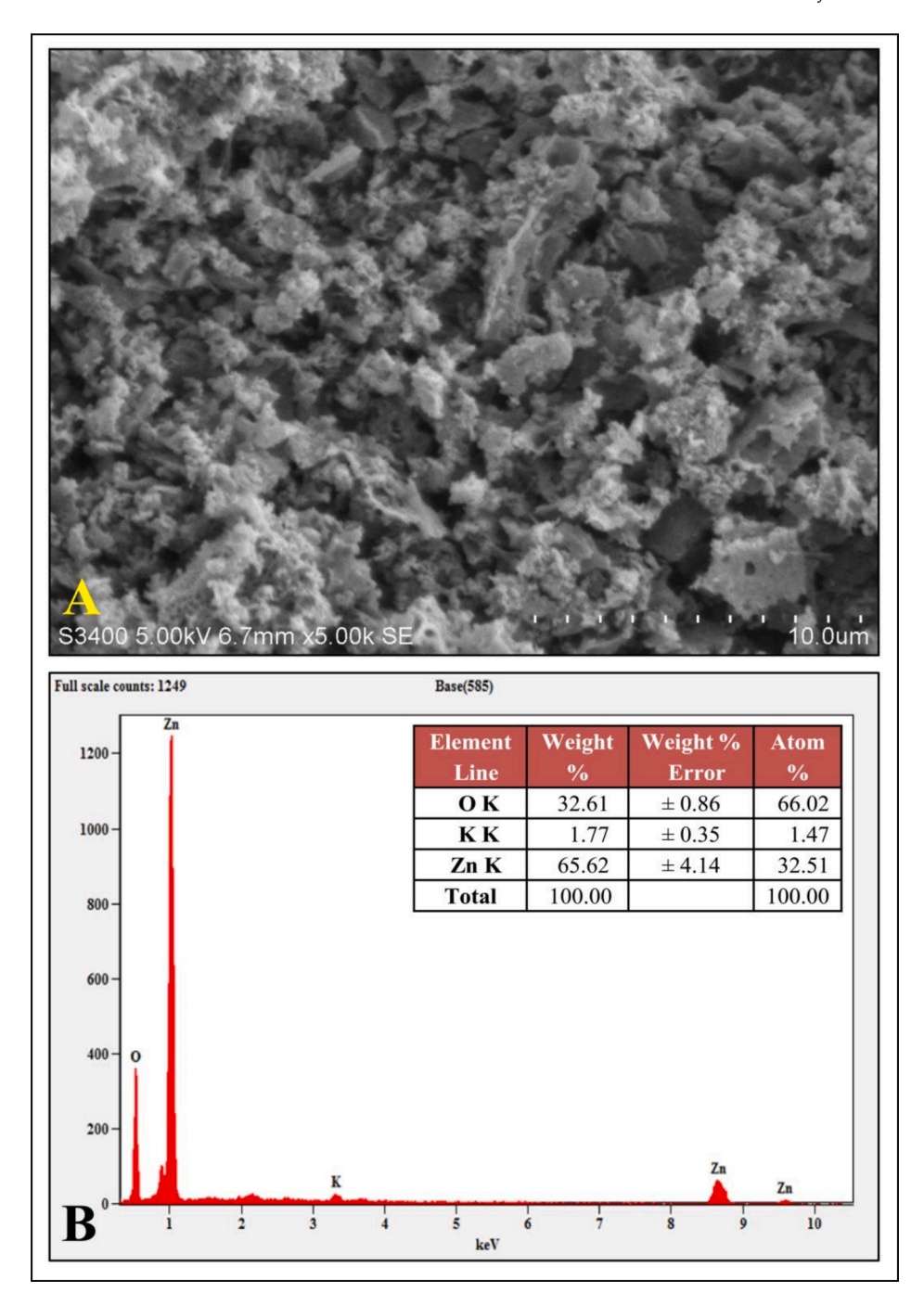


Fig. 3. Scanning Electron Microscopic image (A) and Elemental analysis (B) of phyto-fabricated Bh-ZnO-NPs.

[alcohol/phenol], 2918.67 cm⁻¹ [aliphatic stretch], 1719.85 cm⁻¹ [amides stretch], 1589.76 cm⁻¹ [NH], 1204.96 cm⁻¹ [aromatic amine group], 1024.26 cm⁻¹ [aromatic amine group] was noticed in the plant extract. The spectral results affirmed the involvement of the phyto-constituents during the phyto-fabrication of ZnO-NPs as observed by comparing the spectral results of plant extract and Bh-ZnO-NPs (Fig. 2B). In addition, the presence of adsorption peak in the region of 3250 cm⁻¹ in plant extract and the absence in Bh-ZnO-NPs indicated the particles were free of moisture. Furthermore, it is well-established and supported by the literature that metabolite reduction is followed by capping and stabilization during plant-mediated nanoparticle synthesis [37,38].

The morphology of the nanoparticles observed under the FE-SEM showed agglomeration of the particles (Fig. 3A), while the elemental

investigation revealed that the particles had a ZnO content of 98.23% (Fig. 3B), thereby supporting the results obtained in the XRD studies. Accordingly, the agglomeration of the particles noticed during the study may be attributed to their (Zn⁺) polarity and electrostatic attraction, as reported by Zhang et al. [39]. Similarly, agglomeration in plant-mediated synthesis of ZnO-NPs with greater than 80% purity in the ZnO is noticed by Murali et al. [32] (*Ipomoea obscura*) and Udayashankar et al. [40] (*Passiflora subpeltata*) during their study. The phyto-fabricated ZnO-NPs were examined using transmission electron microscopy (TEM), which revealed the nano-regime as depicted in Fig. 4A. In addition, the SAED pattern revealed the synthesized particles are polycrystalline in nature (Fig. 4B), which matches the XRD peaks (Miller indices). The Fig. 4C depicts the D-spacing and periodic arrangement of ZnO-NPs; the estimated D-spacing value for the sample

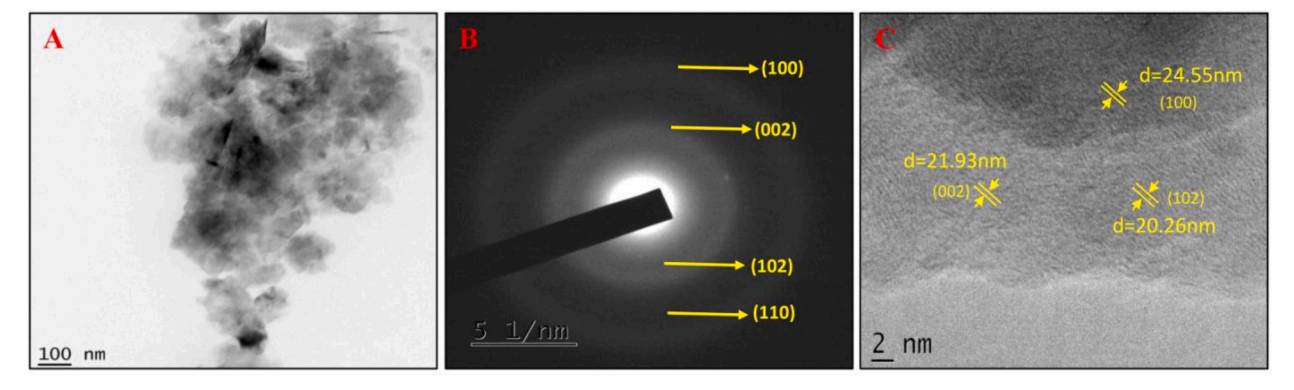


Fig. 4. Transmission Electron Microscopic image of phyto-fabricated Bh-ZnO-NPs (A); TEM image (100 nm) (B) SEAD pattern and (C) HR-TEM (2 nm) with d-spacing.

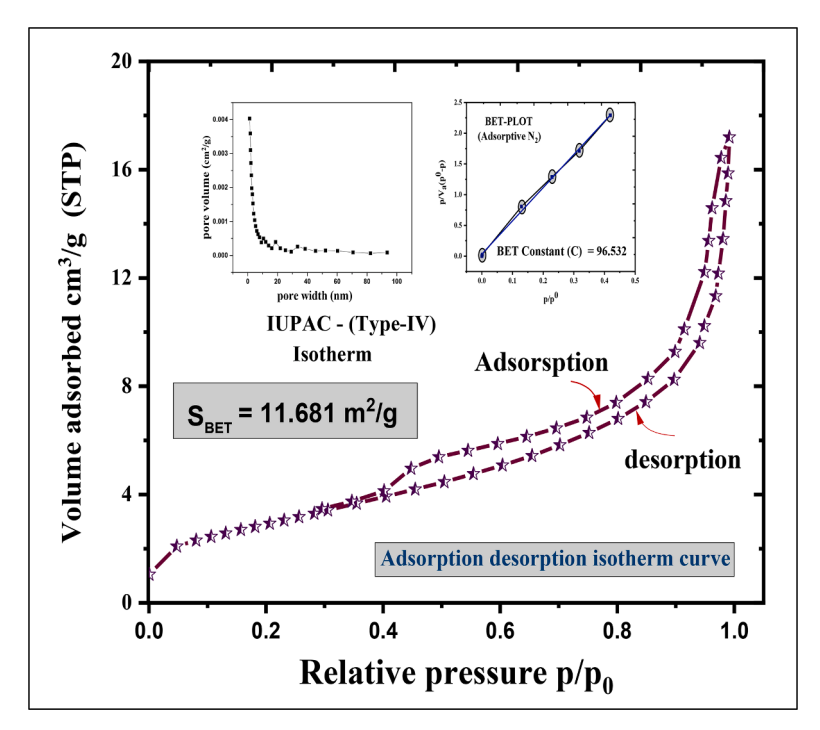


Fig. 5. BET and N_2 adsorption isotherms of phyto-fabricated Bh-ZnO-NPs.

Table 2 Photocatalytic ability of phyto-fabricated Bh-ZnO-NPs and their kinetics.

Concentration of Bh-ZnO-NPs (g L ⁻¹)	Photocatalytic Degradation (%)	Pragmatic kinetic rate constant [k(p)] - (min ⁻¹)	R ² value
0	6.22	0.01248	0.95261
0.25	54.22	0.01361	0.98697
0.50	78.59	0.01523	0.99534
0.75	92.18	0.01648	0.99547
1.00	94.22	0.01654	0.99677

was determined to be 4.29 nm, demonstrating the distinct separation of the inter-planar spacing. The surface area of nanomaterials is noted to be directly proportional to the active site and photocatalytic performance. Photocatalyst with a large surface area has enhanced active sites, assisting during the dye molecules' adsorption and desorption. Similarly, the surface area of the Bh-ZnO-NPs was estimated based on the amount of N_2 absorbed by the sample through BET analyses. For the BET analyses, the Bh-ZnO-NPs were pre-dried at 350 °C for 4 h with a weight of 0.2001 g. The nitrogen desorption/adsorption isotherm confirmed

that the Bh-ZnO-NPs exhibit a similar Type – IV isotherm curve as per IUPAC classification (Fig. 5) [41]. The pore size distributions of Bh-ZnO-NPs plot provided by the BJH method demonstrated that the particles had mesoporous characteristics (insight Fig. 5). Furthermore, the Bh-ZnO-NPssurface area, total pore volume, and mean pore diameter were $11.681~{\rm m}^2{\rm g}^{-1}$, $0.0012632~{\rm cm}^3{\rm g}^{-1}$, (p/po=0.908), and 6.2507 nm, respectively (Suppl. Table 2). The pores in the Bh-ZnO-NPs reveal that the molecules of MR dye may easily enter the inner space of the nanoparticles and then scatter, improving their photocatalytic capabilities, according to the study's findings. In addition the mechanism involved during the synthesis of the Bh-ZnO-NPs is depicted in Fig. 6.

3.2. Antioxidant potential of Bh-ZnO-NPs

The most reactive type of free radicals, the hydroxyl radicals, are to blame for lipid peroxidation and DNA oxidation, which can lead to many diseases and their consequences [42]. The RSA properties of Bh-ZnO-NPs using the DPPH, ABTS, superoxide and $\rm H_2O_2$ methods are presented in Table 1. According to various methodologies, the RSA of *B. hispida* ZnO-NPs produced through green synthesis ranged between

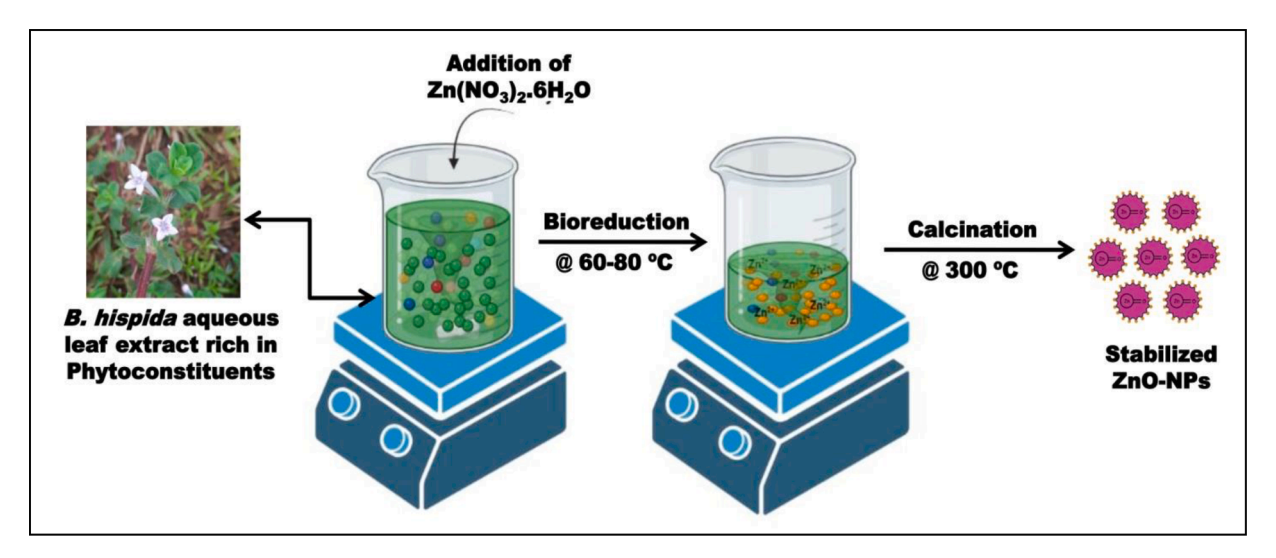


Fig. 6. Mechanism involved during the phyto-fabrication Bh-ZnO-NPs.

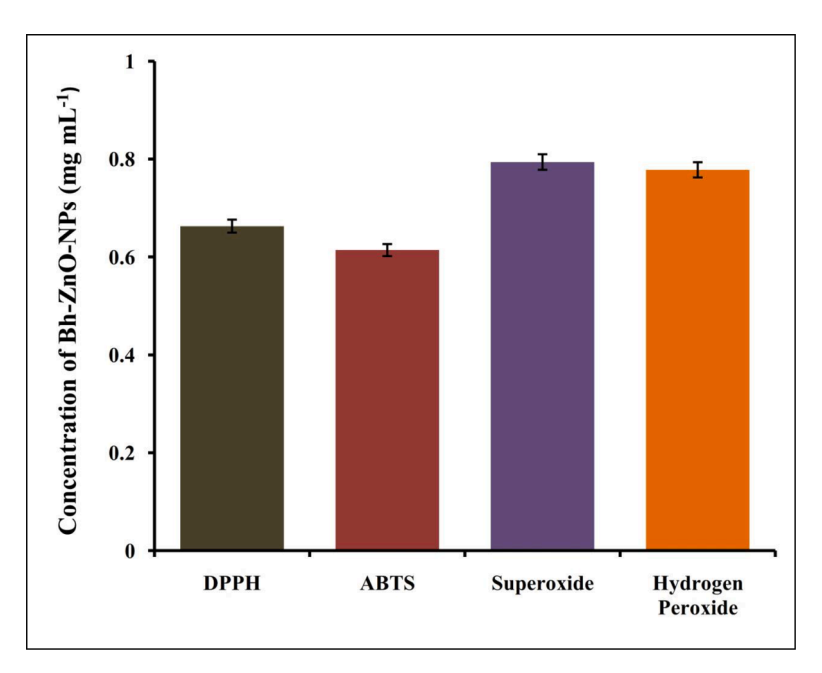


Fig. 7. IC₅₀ concentration of RSA offered by Bh-ZnO-NPs for different methods employed.

4% and 66%, and as Bh-ZnO-NPs concentration increased, so did their antioxidant capacity. Among the methods employed, the half-maximum inhibitory concentrations (IC $_{50}$) of RSA were noticed between 0.6 to 0.8 mg mL $^{-1}$ (Fig. 7), while at 0.05 mg mL $^{-1}$, ascorbic acid, which served as a positive control provided 75% RSA. Similarly, ZnO-NPs synthesized using plant extracts have shown significant antioxidant potential compared to their plant extracts alone [9,37]. Besides, Suresh et al. [21] have also reported that the enhanced RSA of ZnO-NPs synthesized using the plant extracts is ascribed to the encapsulating phyto-constituents during the fabrication of nanoparticles.

3.3. Photocatalytic response of Bh-ZnO-NPs

The photocatalytic degradation potential of MR by the phytofabricated nanoparticles was evaluated with different concentrations (0 to 1 g $\rm L^{-1}$) and time intervals without altering the concentration of dye and pH during the study under both dark and light conditions. From the results, it was noted that the Br-ZnO-NPs caused no substantial photodegradation upon interaction with dye solution under dark. At the

same time, there was a significant increase in the photo-degradation ability of the synthesized nanoparticles when subjected to solar irradiations (Fig. 8A). Among the test concentrations evaluated during the study, a maximum of 94.22% dye degradation (1 g L⁻¹) was noticed after 40 min of solar irradiation with the catalyst Bh-ZnO-NPs (Table 2, Suppl. Fig. 1). In addition, with an increase in the concentration of the catalyst from 0 to 1 g L⁻¹, the rate of deterioration rose linearly (Fig. 8B). The study outcome is in agreement with the outcome of Davar et al. [1] in which plant extract (lemon juice) mediated ZnO-NPs synthesis showed MR dye degradation upon solar irradiation. Further, it is well documented that ZnO has more active sites, which are extremely efficient in the generation of hydrogen peroxide and superior reaction rates [15, 43]. The present study's photo-degradation kinetics of MR dye followed the pseudo-first-order reaction with a rate constant of 0.016 min⁻¹ (Fig. 8C), as the results showed the best linear fit. Previous studies have noted that the kinetics following the best linear fit plot is considered the rate law governing the degradation reaction [44]. Besides, slopes of ln (Ct/Co) plots and the k constants values of samples obtained during the study are depicted in Fig. 8D, while the value of adsorption capacity at

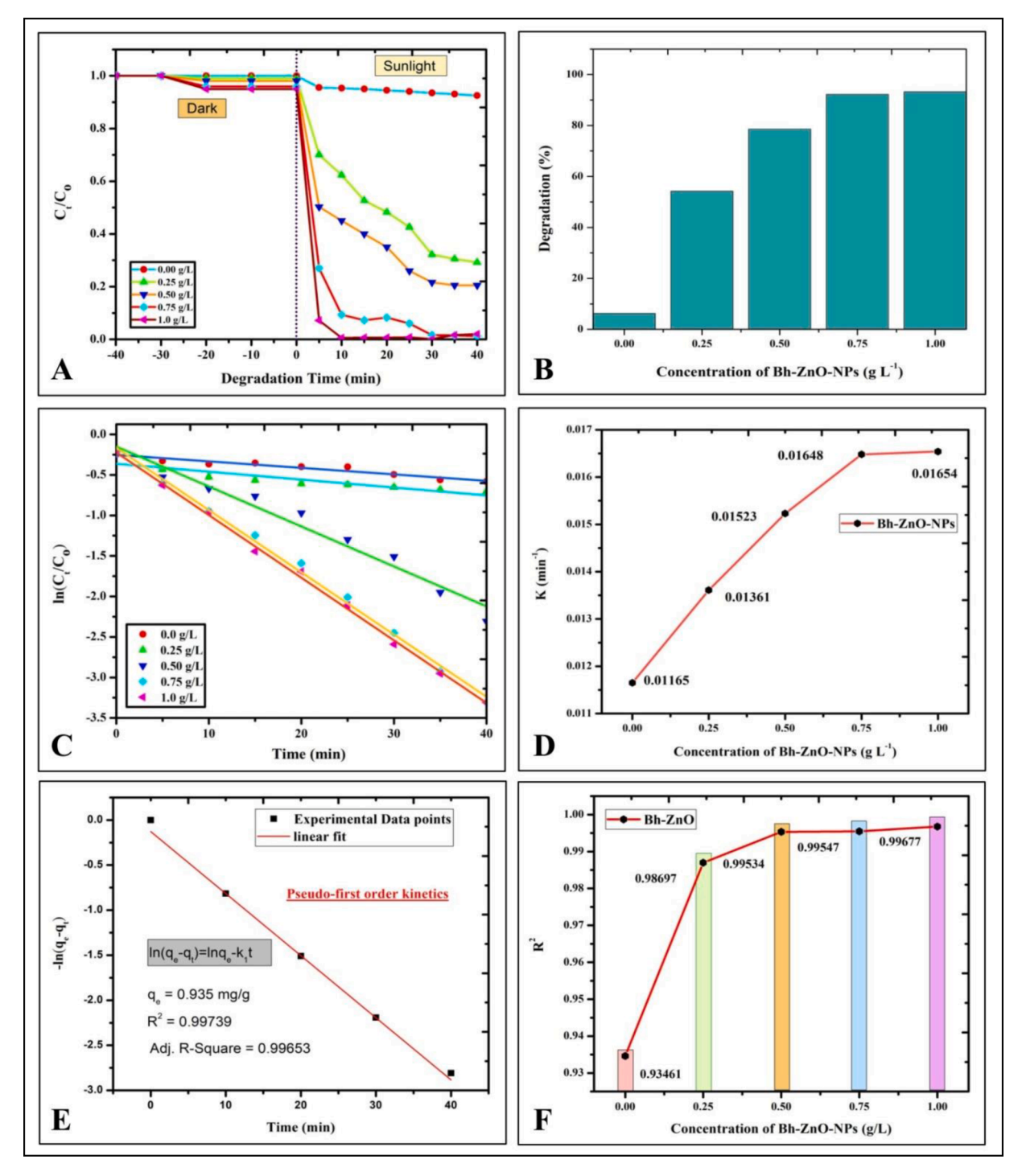


Fig. 8. Photocatalytic ability of phyto-fabricated Bh-ZnO-NPs. A- Photo-degradation studies under dark and simulated solar irradiation conditions; B- Percentage of photo-degradation for MR dye; C- Pseudo-first order kinetic studies; D- Pragmatic rate constant K variation with respect to the concentration of the MR dye; E-Value of adsorption capacity at equilibrium (q_e) by pseudo first order linear fit kinetics; F- R^2 value variation with respect to the concentration of the MR dye.

equilibrium (q_e) 0.935 mg g⁻¹ by pseudo first order linear fit kinetics is provided as Fig. 8E. Besides, R² is one of the selection criteria for the best-fitting model, which predicts the adsorption capacity values at equilibrium and explains the kinetics of the adsorption route by comparing the results to the experimental adsorption capacity [18]. The degradations R² value variation of the present study with respect to the concentration of the MR dye is displayed in Fig. 8F. The obtained results can be corroborated by the concentration dependent increase in photon absorption that leads to the enhanced formation of active catalytic sites

(electrons and holes) for hydroxyl radical generation [45]. Similarly, Anjali et al. [2] have noted that, as the dosage of ZnO-NPs synthesized from the seaweed was increased, more organic pollutants were adsorbed onto the catalyst, thereby contributing towards efficient photo-degradation of MR dye, which conforms to the study's findings. Further, the photo-degradation ability might also be attributed to its ability to absorb light to generate and transfer e^- and h^+ pairs onto the surface leading to redox reactions [46]. In continuation, it is well documented that a reaction involving the holes and water molecules and

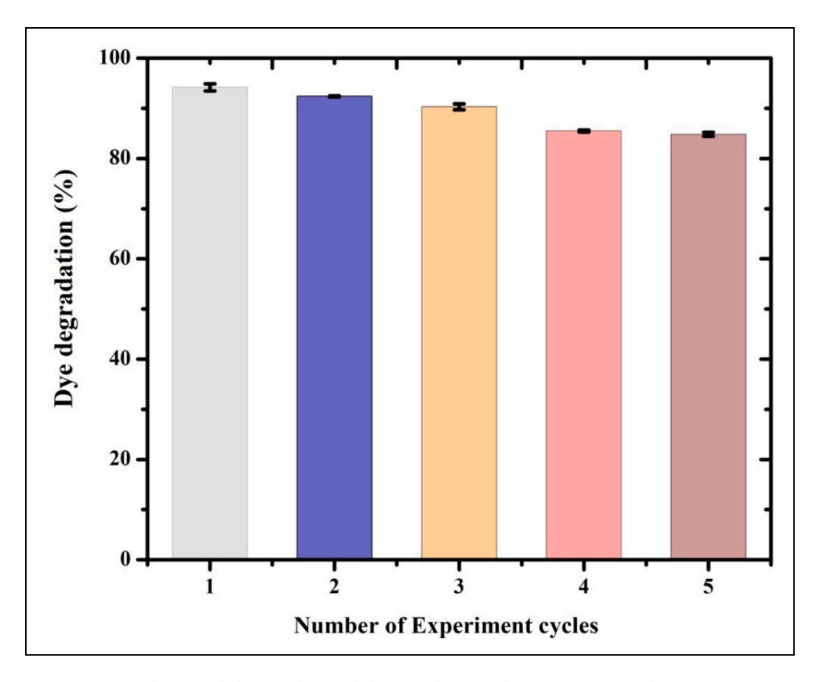


Fig. 9. Photo-stability and reusability studies of phyto-fabricated Bh-ZnO-NPs.

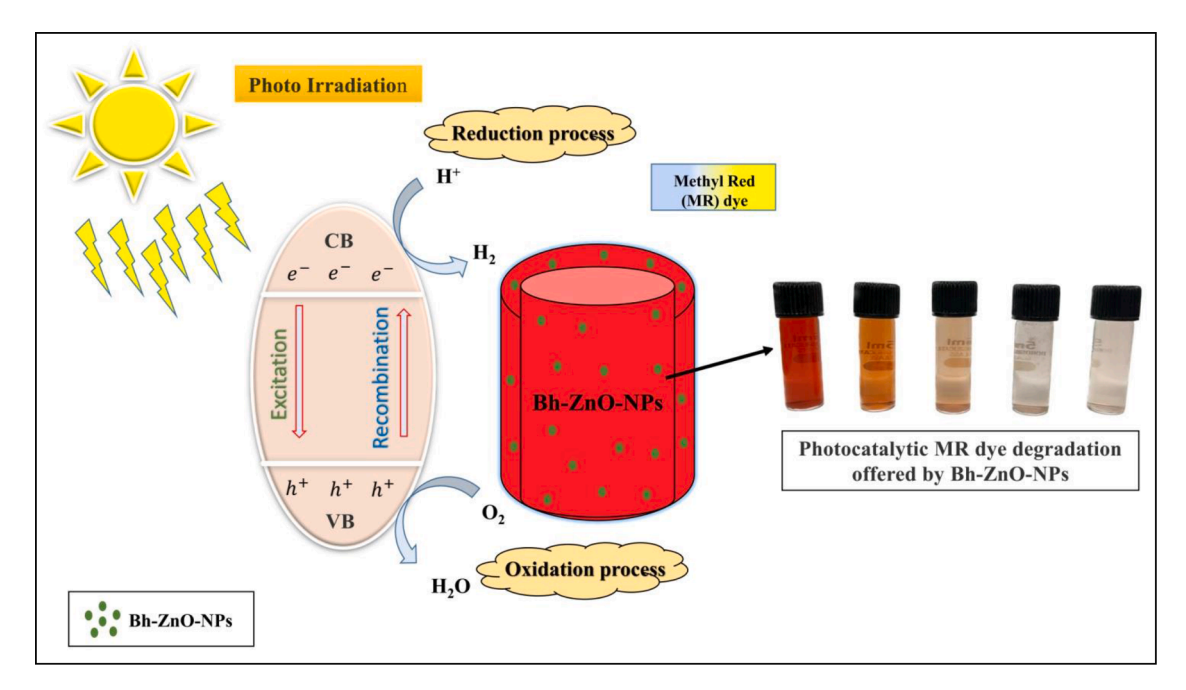


Fig. 10. Plausible mechanism involved during the MR dye degradation by Bh-ZnO-NPs.

between electrons and oxygen results in the formation of extremely reactive hydroxyl radicals and superoxide anions, respectively which are principally in charge of the methyl red dye's breakdown [16,28,45].

3.4. Photo-stability and reusability of phyto-fabricated Bh-ZnO-NPs

The reusability studies using Bh-ZnO-NPs were also carried out for five cycles to note the dye degradation effectiveness of the synthesized particles under solar irradiation (Fig. 9). During the study, the catalyst (Bh-ZnO-NPs) was removed after each cycle by centrifugation and subjected for drying (6 h at 80 $^{\circ}\text{C})$ before use. It was noted that the degradation ability of the Bh-ZnO-NPs was found to be between 94.24% to 84.8% from the first to fifth cycle, respectively. The obtained results signify the effectiveness of Bh-ZnO-NPs for its photo-stability and

reusability even at the last evaluation cycle. Likewise, Anjali et al. [2] and Abhilash et al. [25] reported that ZnO-NPs synthesized from plant extract had photo-stability and reusability application. A schematic representation of the photo-degardation by the catalyst Bh-ZnO-NPs is depicted in Fig. 10. The reduction in MR dye degradation ability by the catalyst after recycling might be ascribed to the unavoidable decline in the revival of the photocatalyst that occurs after each cycle [47]. Additionally, Table 3 highlights the significance of phytofabricated ZnO-NPs and their potential for use as antioxidants and photocatalysts. The table compares the findings of the current investigation and depicts the plant and its part used for the synthesis of ZnO-NPs, as well as the size, morphology, and application of the same.

Table 3Comparison of obtained results of phyto-fabricated Bh-ZnO-NPs with the literature.

Plant Name	Plant Part Used	Zinc Precursor	Size (nm)/ Morphology	Properties	Photocatalytic Reusability	Reference
Eucalyptus globulus	Leaf	Zinc nitrate hexahydrate	11.6/ Spherical	Antioxidant and Photocatalytic	No	Siripireddy and Mandal [48]
Abelmoschus esculentus	Okra mucilage	Zinc acetate dihydrate	29–70/ Spherical & Rod-like	Photocatalytic	No	Prasad et al. [49]
Trianthema portulacastrum	Plant	Zinc sulphate	25–90/ Spherical	Antibacterial, Antifungal, Antioxidant, Anticancer and Photocatalytic	No	Khan et al. [50]
Cyanometra ramiflora	Leaves	Zinc acetate	13.33/ Hexagonal	Photocatalytic	No	Varadavenkatesan et al. [16]
Hippophae rhamnoides	Fruit	Zinc nitrate hexahydrate	17.15	Photocatalytic activity	Yes	Rupa et al. [51]
Mussaenda frondosa	Leaf/ Stem/ Leaf derived callus	Zinc nitrate hexahydrate	8–15/ Hexagonal	Antibacterial, Antioxidant, Antidiabetic, Anticancer, Anti-inflammatory and Photocatalytic	No	Jayappa et al. [52]
Linum usitatissimum	Seeds	Zinc nitrate hexahydrate	40–53/ Spherical	Photocatalytic	No	Alkasir et al. [44]
Aegle marmelos	Juice	Zinc nitrate hexahydrate	~20/ Hexagonal	Antibacterial, Antioxidant and Photocatalytic	No	Mallikarjunaswamy et al. [53]
Sambucus ebulus	Leaf	Zinc acetate dihydrate	25–30/ Spherical	Antibacterial, Antioxidant and Photocatalytic	No	Alamdari et al. [54]
Myristica fragrans	Fruit	Zinc acetate dihydrate	43–83/ Spherical or elliptical	Antibacterial, Antiparasitic, Antioxidant, Antidiabetic, Anticancer and Photocatalytic	No	Faisal et al. [55]
Sida acuta	Leaves	Zinc nitrate hexahydrate	32.82/ Spherical	Antioxidant and Photocatalytic	Yes	Abhilash et al. [25]
Borreria hispida	Leaves	Zinc nitrate hexahydrate	21.87/ Hexagonal	Antioxidant and Photocatalytic	Yes	Present study

4. Conclusion

The study deals with synthesizing zinc oxide nanoparticles using a more environmentally friendly method as the approach avoids many reaction stages, traditional energy sources, hazardous chemicals, quicker and more cost-effective. During the study, Borreria hispida aqueous leaf extract was used for synthesizing zinc oxide nanoparticles for the first time as an eco-friendly approach. According to investigations, the UV-visible spectrum of Bh-ZnO-NPs showed a characteristic peak at 304 nm with 3.45 eV band gap energy. Likewise, according to XRD investigations, the produced Bh-ZnO-NPs had a wurtzite structure. An electron microscope study revealed that the nanoparticles are agglomerated and EDS studies confirmed the ZnO purity of 98.23% in Bh-ZnO-NPs. BET surface area analysis confirmed that the particles exhibited a similar Type - IV isotherm curve as per IUPAC classification with 11.681 m²g⁻¹ and a surface roughness (Ra) value of 6.25 nm. The ZnO nanoparticles' exhibited strong antioxidant properties with an IC_{50} between 0.6 to 0.8 mg mL⁻¹ among the different tests evaluated. Besides, the synthesized Bh-ZnO-NPs also offered effective photocatalytic activity of 94.22% for the photo-degradation of MR with a catalyst dosage of 1 g/L within 40 min under solar irradiation. The photo-stability and reusability studies confirmed that the catalyst (Bh-ZnO-NPs) had an efficacy of 84.8% at the fifth cycle of their reusability. The present research effectively illustrates a simple, affordable, and environmentally friendly way of producing multifunctional ZnO nanoparticles from B. hispida as a promising alternative to the present day chemicals for wastewater treatment with antioxidant potential.

CRediT authorship contribution statement

Abhilash Mavinakere Ramesh: Conceptualization, Formal analysis, Writing – review & editing. Dhananjay Purushotham: Conceptualization, Formal analysis, Writing – review & editing. Anju Kodandaram: Conceptualization, Formal analysis, Writing – review & editing. Natarajamurthy Shilpa: Methodology, Data curation, Writing – review & editing. Sudarshana Brijesh Singh: Methodology, Data curation, Writing – review & editing. Mohammed Aiyaz: Methodology, Data curation, Writing – review & editing. Hittanahallikoppal

Gajendramurthy Gowtham: Software, Writing – review & editing. Abbas Rahdar: Writing – review & editing. Kasinathan Kaviyarasu: Funding acquisition, Investigation, Supervision, Writing – review & editing. Mahadevamurthy Murali: Software, Funding acquisition, Investigation, Supervision, Writing – review & editing.

Declaration of Competing Interest

The authors declare that all data supporting the findings of this study are available in the paper.

Data availability

Data will be made available on request.

Acknowledgments

The authors thank the Botany, Microbiology and Biotechnology departments of the University of Mysore, Mysuru, for facilitating the research.

Supplementary materials

Supplementary material associated with this article can be found, in the online version, at doi:10.1016/j.molstruc.2023.136152.

References

- F. Davar, A. Majedi, A. Mirzaei, Green synthesis of ZnO nanoparticles and its application in the degradation of some dyes, J. Am. Ceram. Soc. 98 (2015) 1739–1746, https://doi.org/10.1111/jace.13467.
- [2] K.P. Anjali, R. Raghunathan, G. Devi, S. Dutta, Photocatalytic degradation of methyl red using seaweed mediated zinc oxide nanoparticles, Biocatal. Agric. Biotechnol. (2022), 102384, https://doi.org/10.1016/j.bcab.2022.102384.
- [3] J. Lin, F. Gulbagca, A. Aygun, R.N.E. Tiri, C. Xia, Q. Van Le, T. Gur, F. Sen, Y. Vasseghian, Phyto-mediated synthesis of nanoparticles and their applications on hydrogen generation on NaBH4, biological activities and photodegradation on azo dyes: development of machine learning model, Food Chem. Toxicol. 163 (2022), 112972, https://doi.org/10.1016/j.fct.2022.112972.

- [4] S. Gunalan, R. Sivaraj, V. Rajendran, Green synthesized ZnO nanoparticles against bacterial and fungal pathogens, Prog. Nat. Sci. 22 (2012) 693–700, https://doi. org/10.1016/j.pnsc.2012.11.015.
- [5] P. Basnet, T.I. Chanu, D. Samanta, S. Chatterjee, A review on bio-synthesized zinc oxide nanoparticles using plant extracts as reductants and stabilizing agents, J. Photochem. Photobiol. B 183 (2018) 201–221, https://doi.org/10.1016/j.iphotobiol.2018.04.036
- [6] M.A. Ansari, M. Murali, D. Prasad, M.A. Alzohairy, A. Almatroudi, M.N. Alomary, A.C. Udayashankar, S.B. Singh, S.M.M. Asiri, B.S. Ashwini, H.G. Gowtham, N. Kalegowda, K.N. Amruthesh, T.R. Lakshmeesha, S.R. Niranjana, Cinnamomum verum bark extract mediated green synthesis of ZnO nanoparticles and their antibacterial potentiality, Biomolecules 10 (2020) 336, https://doi.org/10.3390/biom.10020336.
- [7] H. Seckin, R.N.E. Tiri, I. Meydan, A. Aygun, M.K. Gunduz, F. Sen, An environmental approach for the photodegradation of toxic pollutants from wastewater using Pt–Pd nanoparticles: antioxidant, antibacterial and lipid peroxidation inhibition applications, Environ. Res. 208 (2022), 112708, https://doi.org/10.1016/j.envres.2022.112708.
- [8] M. Murali, A. Thampy, S. Anandan, M. Aiyaz, N. Shilpa, S.B. Singh, H.G. Gowtham, A.M. Ramesh, A. Rahdar, G.Z. Kyzas, Competent antioxidant and antiglycation properties of zinc oxide nanoparticles (ZnO-NPs) phyto-fabricated from aqueous leaf extract of *Boerhaavia erecta* L, Environ. Sci. Pollut. Res. 30 (19) (2023) 56731–56742, https://doi.org/10.1007/s11356-023-26331-8.
- [9] M. Alhujaily, S. Albukhaty, M. Yusuf, M.K. Mohammed, G.M. Sulaiman, H. Al-Karagoly, A.A. Alyamani, J. Albaqami, F.A. AlMalki, Recent advances in plantmediated zinc oxide nanoparticles with their significant biomedical properties, Bioengineering 9 (2022) 541, https://doi.org/10.3390/bioengineering9100541.
- [10] Y. Wu, E.E. Altuner, R.N.E.H. Tiri, M. Bekmezci, F. Gulbagca, A. Aygun, C. Xia, Q. Van Le, F. Sen, H. Karimi-Maleh, Hydrogen generation from methanolysis of sodium borohydride using waste coffee oil modified zinc oxide nanoparticles and their photocatalytic activities, Int. J. Hydrogen Energy 48 (17) (2023) 6613–6623, https://doi.org/10.1016/j.ijhydene.2022.04.177.
- [11] H. Agarwal, S.V. Kumar, S.A. Rajeshkumar, Review on green synthesis of zinc oxide nanoparticles—an eco-friendly approach, Resour. Eff. Technol. 3 (2017) 406–413, https://doi.org/10.1016/j.reffit.2017.03.002.
- [12] T. Rodriguez-Flores, C. Haro-Perez, E.E. Gerardo-Morales, G.E. de la Huerta-Hernandez, L. Gonzalez-Reyes, I. Hernandez-Perez, Influence of precursor concentration in the synthesis of ZnO nanoparticles on their morphological, structural, and photocatalytic properties, Top. Catal. 65 (2022) 1149–1162, https://doi.org/10.1007/s11244-022-01687-2.
- [13] Y. Liang, H. Demir, Y. Wu, A. Aygun, R.N.E. Tiri, T. Gur, Y. Yuan, C. Xia, C. Demir, F. Sen, Y. Vasseghian, Facile synthesis of biogenic palladium nanoparticles using biomass strategy and application as photocatalyst degradation for textile dye pollutants and their in-vitro antimicrobial activity, Chemosphere 306 (2022), 135518, https://doi.org/10.1016/j.chemosphere.2022.135518.
- [14] E.E. Altuner, R.N.E.H. Tiri, A. Aygun, F. Gulbagca, F. Sen, A. Iranbakhsh, F. Karimi, Y. Vasseghian, E.N. Dragoi, Hydrogen production and photocatalytic activities from NaBH4 using trimetallic biogenic PdPtCo nanoparticles: development of machine learning model, Chem. Eng. Res. Des. 184 (2022) 180–190, https://doi.org/10.1016/j.cherd.2022.05.021.
- [15] D. Suresh, P.C. Nethravathi, H. Rajanaika, H. Nagabhushana, S.C. Sharma, Green synthesis of multifunctional zinc oxide (ZnO) nanoparticles using *Cassia fistula* plant extract and their photodegradative, antioxidant and antibacterial activities, Mater. Sci. Semicond. Process. 31 (2015) 446–454, https://doi.org/10.1016/j. mssp.2014.12.023.
- [16] T. Varadavenkatesan, E. Lyubchik, S. Pai, A. Pugazhendhi, R. Vinayagam, R. Selvaraj, Photocatalytic degradation of Rhodamine B by zinc oxide nanoparticles synthesized using the leaf extract of *Cyanometra ramiflora*, J. Photochem. Photobiol. B 199 (2019), 111621, https://doi.org/10.1016/j. iphotobiol.2019.111621.
- [17] M. Murali, N. Kalegowda, H.G. Gowtham, M.A. Ansari, M.N. Alomary, S. Alghamdi, N. Shilpa, S.B. Singh, M.C. Thriveni, M. Aiyaz, N. Angaswamy, Plant-mediated zinc oxide nanoparticles: advances in the new millennium towards understanding their therapeutic role in biomedical applications, Pharmaceutics 13 (2021) 1662, https://doi.org/10.3390/pharmaceutics13101662.
- [18] M.A. Fagier, Plant-mediated biosynthesis and photocatalysis activities of zinc oxide nanoparticles: a prospect towards dyes mineralization, J. Nanotechnol. 2021 (2021), 6629180, https://doi.org/10.1155/2021/6629180.
- [19] D. Liu, W. Wu, Y. Qiu, S. Yang, S. Xiao, Q.Q. Wang, L. Ding, J. Wang, Surface functionalization of ZnO nanotetrapods with photoactive and electroactive organic monolayers, Langmuir 24 (2008) 5052–5059, https://doi.org/10.1021/la800074f.
- [20] A.K. Sidhu, N. Verma, P. Kaushal, Role of biogenic capping agents in the synthesis of metallic nanoparticles and evaluation of their therapeutic potential, Front. Nanotechnol. 3 (2022), 801620, https://doi.org/10.3389/fnano.2021.801620.
- [21] D. Suresh, R.M. Shobharani, P.C. Nethravathi, M.P. Kumar, H. Nagabhushana, S. C. Sharma, *Artocarpus gomezianus* aided green synthesis of ZnO nanoparticles: luminescence, photocatalytic and antioxidant properties, Spectrochim. Acta A 141 (2015) 128–134, https://doi.org/10.1016/j.saa.2015.01.048.
- [22] J.B. Kavya, M. Murali, S. Manjula, G.L. Basavaraj, M. Prathibha, S.C. Jayaramu, K. N. Amruthesh, Genotoxic and antibacterial nature of biofabricated zinc oxide nanoparticles from Sidarhombifolia Linn, J. Drug Deliv. Sci. Technol. 60 (2020), 101982, https://doi.org/10.1016/j.jddst.2020.101982, 101982.
- [23] M. Murali, S. Anandan, M.A. Ansari, M.A. Alzohairy, M.N. Alomary, S.M.M. Asiri, A. Almatroudi, M.C. Thriveni, S. Brijesh Singh, H.G. Gowtham, M. Aiyaz, S. Chandrashekar, A. Urooj, K.N. Amruthesh, Genotoxic and cytotoxic properties of zinc oxide nanoparticles phyto-fabricated from the obscure morning glory plant

- *Ipomoea obscura* (L.) Ker Gawl, Molecules 26 (2021) 891, https://doi.org/10.3390/molecules26040891.
- [24] J. Ahmed, A. Thakur, A. Goyal, in: Chemistry in the Environment: Biological Treatment of Industrial Wastewater, The Royal Society of Chemistry, UK, 2021, pp. 1–14, https://doi.org/10.1039/9781839165399-00001.
- [25] M.R. Abhilash, K. Pal, A. Kodandaram, B.L. Manjula, D.K. Ravishankar, H. G. Gowtham, M. Murali, A. Rahdar, G.Z. Kyzas, Antioxidant and photocatalytic properties of zinc oxide nanoparticles phyto-fabricated using the aqueous leaf extract of *Sida acuta*, Green Process. Synth. 11 (2022) 857–867, https://doi.org/10.1515/gps-2022-0075.
- [26] R. Kishor, R.N. Bharagava, G. Saxena, Industrial wastewaters: the major sources of dye contamination in the environment, ecotoxicological effects, and bioremediation approaches. Recent Advances in Environmental Management, CRC Press, Boca Raton, FL, USA, 2018, pp. 1–25..
- [27] E.A.S. Dimapilis, C.S. Hsu, R.M.O. Mendoza, M.C. Lu, Zinc oxide nanoparticles for water disinfection, Sustain. Environ. Res. 28 (2018) 47–56, https://doi.org/ 10.1016/j.seri.2017.10.001.
- [28] J. Gangwar, J.K. Sebastian, Unlocking the potential of biosynthesized zinc oxide nanoparticles for degradation of synthetic organic dyes as wastewater pollutants, Water Sci. Technol. 84 (2021) 3286–3310, https://doi.org/10.2166/wst.2021.430.
- [29] V. Meti, K. Chandrashekar, Shishir Mishra, Pharmacological activities of Spermacocehispida Linn: a review, Int. J. Res. Ayurveda Pharm. 4 (2013) 18–22, https://doi.org/10.7897/2277-4343.04115.
- [30] R.L. Sundaram, H.R. Vasanthi, Spermacocehispida Linn: a critical review on pharmacognosy, phytochemistry, and pharmacology based on traditional claims, Phytomed. Plus 2 (2022), 100143, https://doi.org/10.1016/j. phyplu.2021.100143.
- [31] R. Venugopalan, S. Pitchai, K. Devarayan, V.C. Swaminathan, Biogenic synthesis of copper nanoparticles using *Borreria hispida* (Linn.) extract and its antioxidant activity, Mater. Today 33 (2020) 4023–4025, https://doi.org/10.1016/j. matpr.2020.06.419.
- [32] M. Murali, C. Mahendra, N. Nagabhushan, Rajashekar, M.S. Sudarshana, K. A. Raveesha, K.N. Amruthesh, Antibacterial and antioxidant properties of biosynthesized zinc oxide nanoparticles from *Ceropegia candelabrum* L.—an endemic species, Spectrochim. Acta A 179 (2017) 104–109, https://doi.org/10.1016/j.saa.2017.02.027.
- [33] N.K. Hemanth Kumar, M. Murali, A. Satish, S. Brijesh Singh, H.G. Gowtham, H. M. Mahesh, T.R. Lakshmeesha, K.N. Amruthesh, S Jagannath, Bioactive and biocompatible nature of green synthesized zinc oxide nanoparticles from *Simarouba glauca* DC.: an endemic plant to Western Ghats, India, J. Clust. Sci. 31 (2020) 523–534, https://doi.org/10.1007/s10876-019-01669-7.
- [34] S.K. Lakhera, R. Venkataramana, A. Watts, M. Anpo, B. Neppolian, Facile synthesis of Fe₂O₃/Cu₂O nanocomposite and its visible light photocatalytic activity for the degradation of cationic dyes, Res. Chem. Intermed. 43 (2017) 5091–5102, https://doi.org/10.1007/s11164-017-3050-0.
- [35] G. Sharmila, C. Muthukumaran, K. Sandiya, S. Santhiya, R.S. Pradeep, N.M. Kumar, N. Suriyanarayanan, M. Thirumarimurugan, Biosynthesis, characterization, and antibacterial activity of zinc oxide nanoparticles derived from *Bauhinia tomentosa* leaf extract, J. Nanostruct. Chem. 8 (2018) 293–299, https://doi.org/10.1007/ s40097-018-0271-8
- [36] V. Srivastava, D. Gusain, Y.C. Sharma, Synthesis, characterization and application of zinc oxide nanoparticles (n-ZnO), Ceram. Int. 39 (2013) 9803–9808, https://doi. org/10.1016/j.ceramint.2013.04.110.
- [37] Stan et al., 2016; Stan, M., Popa, A., Toloman, D., Silipas, T.D., Vodnar, D.C., 2016. Antibacterial and antioxidant activities of ZnO nanoparticles synthesized using extracts of Allium sativum, Rosmarinus officinalis and Ocimumbasilicum. Acta Metall. Sin. 29, 228–236. 10.1007/s40195-016-0380-7.
- [38] M. Murali, S. Manjula, N. Shilpa, D.K. Ravishankar, C.S. Shivakumara, A. Thampy, A. Ayeshamariam, S. Pandey, S. Anandan, K.N. Amruthesh, F.A. Al-Mekhlafi, K. Kaviyarasu, Facile synthesis of ZnO-NPs from yellow creeping daisy (Sphagneticolatrilobata L.) attenuates cell proliferation by inducing cellular level apoptosis against colon cancer, J. King Saud Univ. Sci. 34 (2022), 102084, https://doi.org/10.1016/j.jksus.2022.102084.
- [39] J. Zhang, L.D. Sun, Y.J. Lin, H. Su, C. Liao, C. Yan, Control of ZnO morphology via a simple solution route, Chem. Mater. 14 (2002) 4172–4177, https://doi.org/ 10.1021/cm020077h.
- [40] A.C. Udayshankar, A.B. Shivaram, M. Murali, T.R. Lakshmeesha, S.G. Lalitha, N. K. Hemanth Kumar, A. Satish, S. Brijesh Singh, G.C. Eswaraiah, S.R. Niranjana, Biosynthesis of zinc oxide nanoparticles using leaf extract of *Passiflora subpeltata*: characterization and Antibacterial activity against *Escherichia coli* isolated from poultry faeces, J. Clust. Sci. 32 (2021) 1663–1672, https://doi.org/10.1007/s10876-020-01926-0.
- [41] A.N. Okte, D. Karamanis, A novel photoresponsive ZnO-flyash nanocomposite for environmental and energy applications, Appl. Catal. B 142 (2013) 538–552, https://doi.org/10.1016/j.apcatb.2013.05.045.
- [42] M. Sharifi-Rad, N.V. Anil Kumar, P Zucca, E.M Varoni, L Dini, E. Panzarini, J. Rajkovic, P.V. TsouhFokou, E Azzini, I Peluso, A Prakash Mishra, Lifestyle, oxidative stress, and antioxidants: back and forth in the pathophysiology of chronic diseases, Front. Physiol. 11 (2020) 694, https://doi.org/10.3389/ fphys.2020.00694.
- [43] P. Peerakiatkhajohn, T. Butburee, J.H. Sul, S. Thaweesak, J.H. Yun, Efficient and rapid photocatalytic degradation of methyl orange dye using Al/ZnO nanoparticles, Nanomaterials 11 (2021) 1059, https://doi.org/10.3390/ nano11041059.
- [44] M. Alkasir, N. Samadi, Z. Sabouri, Z. Mardani, M. Khatami, M. Darroudi, Evaluation cytotoxicity effects of biosynthesized zinc oxide nanoparticles using

- aqueous *Linum usitatissimum* extract and investigation of their photocatalytic activity, Inorg. Chem. Commun. 108066 (2020), https://doi.org/10.1016/j.inoche.2020.108066.
- [45] I.J. Ani, U.G. Akpan, M.A. Olutoye, B.H. Hameed, Photocatalytic degradation of pollutants in petroleum refinery wastewater by TiO₂-and ZnO-based photocatalysts: recent development, J. Clean. Prod. 205 (2018) 930–954, https:// doi.org/10.1016/j.jclepro.2018.08.189.
- [46] V. Batra, I. Kaur, D. Pathania, V. Chaudhary, Efficient dye degradation strategies using green synthesized ZnO-based nanoplatforms: a review, Appl. Surf. Sci. Adv. 11 (2022), 100314, https://doi.org/10.1016/j.apsadv.2022.100314.
- [47] T. Khalafi, F. Buazar, K. Ghanemi, Phycosynthesis and enhanced photocatalytic activity of zinc oxide nanoparticles toward organosulfur pollutants, Sci. Rep. 9 (2019) 6866, https://doi.org/10.1038/s41598-019-43368-3.
- [48] B. Siripireddy, B.K. Mandal, Facile green synthesis of zinc oxide nanoparticles by Eucalyptus globulus and their photocatalytic and antioxidant activity, Adv. Powder Technol. 28 (2017) 785–797, https://doi.org/10.1016/j.apt.2016.11.026.
- [49] A.R. Prasad, J. Garvasis, S.K. Oruvil, A. Joseph, Bio-inspired green synthesis of zinc oxide nanoparticles using *Abelmoschus esculentus* mucilage and selective degradation of cationic dye pollutants, J. Phys. Chem. Solids 127 (2019) 265–274, https://doi.org/10.1016/j.jpcs.2019.01.003.
- [50] Z.U.H. Khan, H.M. Sadiq, N.S. Shah, A.U. Khan, N. Muhammad, S.U. Hassan, K. Tahir, S.Z. Safi, F.U. Khan, M. Imran, N. Ahmad, F. Ullah, A. Ahmad, M. Sayed, M.S. Khalid, S.A. Qaisrani, M. Ali, A. Zakir, Greener synthesis of zinc oxide nanoparticles using *Trianthema portulacastrum* extract and evaluation of its

- photocatalytic and biological applications, J. Photochem. Photobiol. B. Biol. 192 (2019) 147–157, https://doi.org/10.1016/j.jphotobiol.2019.01.013.
- [51] E.J. Rupa, L. Kaliraj, S. Abid, D.C. Yang, S.K.J. Oop, Synthesis of a zinc oxide nanoflower photocatalyst from sea buckthorn fruit for degradation of industrial dyes in wastewater treatment, Nanomaterials 9 (2019) 12, https://doi.org/ 10.3390/nano9121692.
- [52] M.D. Jayappa, C.K. Ramaiah, M.A.P. Kumar, D. Suresh, A. Prabhu, R.P. Devasya, S. Sheikh, Green synthesis of zinc oxide nanoparticles from the leaf, stem and in vitro grown callus of *Mussaenda frondosa* L.: characterization and their applications, Appl. Nanosci. 10 (2020) 3057–3074, https://doi.org/10.1007/s13204-020-01382-2.
- [53] C. Mallikarjunaswamy, V. Lakshmi Ranganatha, R. Ramu, G. Udayabhanu, Nagaraju, Facile microwave-assisted green synthesis of ZnO nanoparticles: application to photodegradation, antibacterial and antioxidant, J. Mater. Sci. 31 (2020) 1004–1021, https://doi.org/10.1007/s10854-019-02612-2.
- [54] S. Alamdari, M.S. Ghamsari, C. Lee, W. Han, H.H. Park, M.J. Tafreshi, H. Afarideh, M.H.M. Ara, Preparation and characterization of Zinc oxide nanoparticles using leaf extract of Sambucus ebulus, Appl. Sci. 10 (2020) 3620, https://doi.org/ 10.3390/appl0103620.
- [55] S. Faisal, H. Jan, S.A. Shah, S. Shah, A. Khan, M.T. Akbar, M. Rizwan, F. Jan, N. Wajidullah, Akhtar, A. Khattak, S. Syed, Green synthesis of Zinc oxide (ZnO) nanoparticles using aqueous fruit extracts of *Myristica fragrans*: their characterizations and biological and environmental applications, ACS Omega 6 (14) (2021) 9709–9722, https://doi.org/10.1021/acsomega.1e00310.